International Journal of Engineering & Technology, 7 (4.28) (2018) 143-150

International Journal of Engineering & Technology

Website: www.sciencepubco.com/index.php/IJET

Research paper

Effects of thermal radiation on electrical MHD flow of nanofluid over stretching sheet

Yahaya Shagaiya Daniel[1], Zuhaila Ismail[2]*, Zainal Abdul Aziz[3] , Faisal Salah[4]

[1,2,3]*Department of Mathematical sciences, Faculty of Science, Universiti Teknologi Malaysia, 81310 UTM Johor Bahru, Johor, Malaysia*
[1,2,3]*UTM Centre for Industrial and Applied Mathematics,*
Universiti Teknologi Malaysia, 81310 UTM Johor Bahru, Johor, Malaysia
[4]*Department of Mathematics, Faculty of Science, University of Kordofan, Elobied, 51111, Sudan.*
[5]*Department of Mathematics, Faculty of Science, Kaduna State University, Kaduna State, Nigeria.*
**Corresponding author E-mail: zuhaila@utm.my*

Abstract

The purpose of this investigation focuses on combined effects of thermal radiation, viscous dissipation and chemical reaction on unsteady magnetohydrodynamic (MHD) natural convection flow and heat transfer of nanofluid over a permeable stretching sheet with electric field effects. The governing equations are partial differential equations, converted to a couple of ordinary differential equations and then solved using implicit finite difference scheme. The electrical conducting nanofluid volume nanoparticle fraction on the boundary is passively rather than actively controlled. The effects of the emerging parameters on the electrical conducting nanofluid velocity, temperature, and nanoparticles concentration volume fraction with skin friction characteristics are examined with the aids of graphs and tabular form and then discussed extensively. Electric field enhances the nanofluid velocity which resolved the sticky effects caused by the magnetic field which suppressed the profiles. Radiative heat transfer and viscous dissipation are sensitive to an increase in the fluid temperature and thicker thermal boundary layer thickness. The nanoparticles concentration enhance with generative chemical reaction while opposite trend occurs for destructive chemical reaction. Comparison with published results is examined and presented which are found to be in good agreement.

Keywords: *MHD nanofluid; thermal radiation; chemical reaction; electric field; stretching sheet.*

1. Introduction

Nanofluid is a heat transfer fluid containing a base fluid and nanoparticles [1]. Application of additives is a technique to enhance the thermal conductivity and the convective heat transfer enactment of the pedestal fluids. The pedestal fluids thermal conductivity is not sufficient adequate to meet with the cooling rate expectation. Recently nanofluids exponential increase in the thermal conductivity and convective heat transfer performance of the pedestal fluids is beyond theory [2-5]. Among the mechanism employed for the intensification in thermal conductivity of nanoliquid are the Brownian motion and thermophoresis of the nanoparticles exclusive the conventional liquids which are considered to be very crucial [6-12]. Magnetic nanofluid contains the liquid and magnetic properties. Different physical properties of these fluids can be tuned through the varying magnetic field. Nanofluid is the suspensions of ultrafine nanoparticles in pedestal fluids that exhibits an exponential increase of their features at modest nanoparticle concentrations. The magnetic nanofluids are manipulated with applied magnetic field [13], which is applicable in a verity of nuclear reactor designs purpose [14], to ensure safety and improved values via economies seen in nuclear power industry [15] which also resolved the difficulties in insufficient energy in supply [16, 17]. Due to stretching sheet, it has a wide application such as metallurgy, polymer engineering, polymerization, and petrochemical industry, features of polymers and structure, processing of polymers and compounding, characteristics of polymers and description of main polymers [16, 18-23].

Thermal radiation has an essential role in the whole heat transfer process due to surface especially when the heat transfer coefficient due to convection is insignificant. It plays a major role in regulatory the heat transfer mechanism in manufacturing industries such as polymer processing. The consequence of thermal radiation becomes imperative that draw the attention of different researchers due to wider coverage in applications [24-31].

A careful review on existing literature materials shown that no work devoted to the investigation on combined effects of thermal radiation, viscous dissipation, the chemical reaction on natural convection of unsteady electrical Magnetohydrodynamics (MHD) nanofluid and heat transfer flow through means of revised Buongiorno model [10] yet. Inspire with these facts, the current investigation analyzes the flow of incompressible nanofluid flow due to stretching sheet in the presence of thermal radiation, electric and magnetic fields, viscous dissipation, and chemical reaction. The converted higher order set of ordinary differential equations from the constitutive governing equations are resolved numerically with aids of Keller box method [32]. The computational are evaluated and examined for dissimilar emerging parameters of the study such as the suction/injection, magnetic field, electric field, unsteadiness parameter, thermal radiation, Grashof number, mass Grashof number, Brownian motion, thermophoresis, Lewis number, and chemical reaction on heat and mass transfer characteristics through tabular forms and graphs.

2. Mathematical formulation

Consider a two-dimensional unsteady natural convection flow of electrical magnetohydrodynamic (MHD) nanofluid due to a linearly stretching sheet. The velocity of the stretching sheet is denoted as $u_w(x,t) = bx/(1-at)$ where b is the stretching rate and a represent the constant having dimension (time)$^{-1}$ such as $(at<1, a\geq 0)$. The boundary layer equations of the fluid flow are consist of the continuity equation, the momentum equation, energy equation and concentration equation, the flow equation is formulated based on Maxwell's equation, Ohm's law in the presence of electrical Magnetohydrodynamics (MHD). The flow is due to stretching sheet medium as results of slot through two equal with associated opposite force and thermally radiative. The magnetic and electric fields conform the Ohm's law express $\bar{J} = \sigma(\bar{E} + \bar{V} \times \bar{B})$ where $\bar{J}$ is denote Joule current, σ is represent electrical conductivity and $\bar{V}$ indicate fluid velocity. The magnetic and electric fields of strength define as $B = B_0/\sqrt{1-at}$ and $E = E_0/\sqrt{1-at}$ are applied normal to the momentum field, such that magnetic Reynolds number is insignificant [9, 33, 34]. Consequently, the induced magnetic field is very smaller compared to applied magnetic field. Hence, induced magnetic field is absence for insignificant magnetic Reynolds number. We choose the Cartesian coordinate system such that x is chosen along the stretching sheet and $y-$axis denotes the normal to the stretching sheet, u and v are the velocity components of the fluid in the x and $y-$direction see Figure 1. Assuming the nanofluid flow to be unsteady two-dimensional boundary layer flow, incorporating Brownian movement for nanofluid and thermophoresis (mass diffusion), the viscous dissipation in the thermal equation and chemical reaction in the concentration equation. The investigation of the nanofluid which involves nanoparticles and liquid. The fluid properties are indicated with subscript as $(\rho c)_f$ and that of particles properties as $(\rho c)_p$. The two-dimensional electrical magnetohydrodynamic natural convection flow governing equations of the incompressible nanofluid are given:

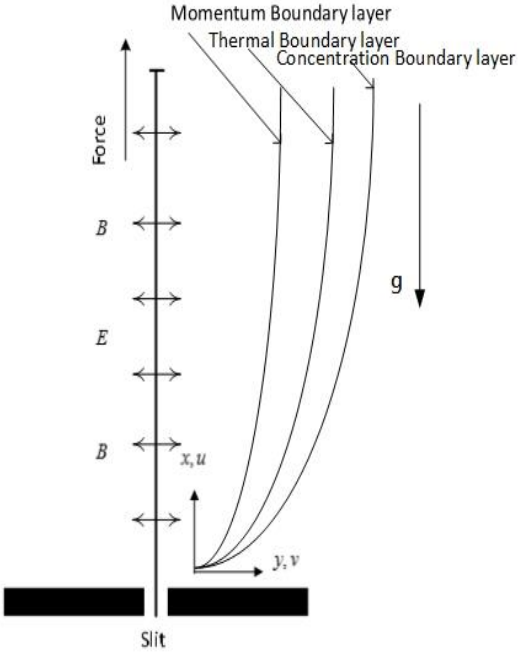

Figure 1 Physical configuration of the geometry

Continuity equation

$$\frac{\partial u}{\partial x} + \frac{\partial v}{\partial y} = 0 \tag{1}$$

$x-$ Momentum equation

$$\frac{\partial u}{\partial t} + u\frac{\partial u}{\partial x} + v\frac{\partial u}{\partial y} = -\frac{1}{\rho_f}\frac{\partial p}{\partial x} + \nu\left(\frac{\partial^2 u}{\partial x^2} + \frac{\partial^2 u}{\partial y^2}\right) + \frac{\sigma}{\rho_f}\left(EB - uB^2\right) + \frac{1}{\rho_f}\left[(1-\varphi_\infty)\rho_{f\infty}\beta_T(T-T_\infty) + (\rho_p - \rho_{f\infty})\beta_\varphi(\varphi-\varphi_\infty)\right]g \tag{2}$$

$y-$ Momentum equation

$$\frac{\partial v}{\partial t} + u\frac{\partial v}{\partial x} + v\frac{\partial v}{\partial y} = -\frac{1}{\rho_f}\frac{\partial p}{\partial y} + \nu\left(\frac{\partial^2 v}{\partial x^2} + \frac{\partial^2 v}{\partial y^2}\right) \tag{3}$$

Energy equation

$$\frac{\partial T}{\partial t} + u\frac{\partial T}{\partial x} + v\frac{\partial T}{\partial y} = \frac{k}{(\rho c)_f}\left(\frac{\partial^2 T}{\partial x^2} + \frac{\partial^2 T}{\partial y^2}\right) - \frac{1}{(\rho c)_f}\left(\frac{\partial q_r}{\partial y}\right) + \frac{\mu}{(\rho c)_f}\left(\frac{\partial u}{\partial y}\right)^2 + \tau\left\{D_B\left(\frac{\partial \varphi}{\partial x}\frac{\partial T}{\partial x} + \frac{\partial \varphi}{\partial y}\frac{\partial T}{\partial y}\right) + \frac{D_T}{T_\infty}\left[\left(\frac{\partial T}{\partial x}\right)^2 + \left(\frac{\partial T}{\partial y}\right)^2\right]\right\} + \frac{\sigma}{(\rho c)_f}(uB - E)^2 \tag{4}$$

Concentration equation

$$\frac{\partial \varphi}{\partial t} + u\frac{\partial \varphi}{\partial x} + v\frac{\partial \varphi}{\partial y} = D_B\left(\frac{\partial^2 \varphi}{\partial x^2} + \frac{\partial^2 \varphi}{\partial y^2}\right) + \frac{D_T}{T_\infty}\left(\frac{\partial^2 T}{\partial x^2} + \frac{\partial^2 T}{\partial y^2}\right) - k_1(\varphi - \varphi_\infty) \tag{5}$$

The boundary conditions at the sheet for the physical model are presented by

$$y = 0: u = u_w(x,t),\ v = v_w(x,t),\ T = T_w(x,t),\ D_B\frac{\partial \varphi}{\partial y} + \frac{D_T}{T_\infty}\frac{\partial T}{\partial y} = 0,$$
$$y \to 0: \quad u \to 0, \quad T \to T_\infty, \quad \varphi \to \varphi_\infty, \tag{6}$$

Here $v_w = -v_0/\sqrt{1-at}$ is the wall mass transfer, when $v_w < 0$ denote the injection while $v_w > 0$ indicates the suction. Where u and v represent the velocity components along the x and $y-$axis respectively. The $p, \alpha = k/(\rho c)_f, \mu, \rho, \rho_f,$ and ρ_p is for the fluid pressure, the thermal diffusivity, the kinematic viscosity, the density, the fluid density and particles density respectively. We also have $D_B, D_T, \tau = (\rho c)_p/(\rho c)_f$ which represents the Brownian diffusion coefficient, the thermophoresis diffusion coefficient, the ratio between the effective heat transfer capacity of the ultrafine nanoparticle material and the heat capacity of the fluid and the rate of chemical reaction is $k_1 = k_0/(1-at)$ respectively.

The radiative heat flux q_r by means of Rosseland approximation discussed in [35] is applied to equation (4), such that.

$$q_r = -\frac{4\sigma^*}{3k^*}\frac{\partial T^4}{\partial y} \tag{7}$$

Where σ^* represent the Stefan-Boltzmann constant and k^* denote the mean absorption coefficient. Expanding T^4 by using Taylor's series about T_∞ and neglecting higher order terms, we have,

$$T^4 \cong 4T_\infty^3 T - 3T_\infty^4 \tag{8}$$

Using equation (8) into equation (7), we get

$$\frac{\partial q_r}{\partial y} = -\frac{16T_\infty^3\sigma^*}{3k^*}\frac{\partial^2 T}{\partial y^2} \tag{9}$$

Use equation (9) in equation (4), we obtain

$$\frac{\partial T}{\partial t}+u\frac{\partial T}{\partial x}+v\frac{\partial T}{\partial y}=\frac{k}{(\rho c)_f}\left(1+\frac{16\sigma^* T_\infty^3}{3k^* k}\right)\left(\frac{\partial^2 T}{\partial x^2}+\frac{\partial^2 T}{\partial y^2}\right)+\frac{\mu}{(\rho c)_f}\left(\frac{\partial u}{\partial y}\right)^2+$$
$$\tau\left\{D_B\left(\frac{\partial \varphi}{\partial x}\frac{\partial T}{\partial x}+\frac{\partial \varphi}{\partial y}\frac{\partial T}{\partial y}\right)+\frac{D_T}{T_\infty}\left[\left(\frac{\partial T}{\partial x}\right)^2+\left(\frac{\partial T}{\partial y}\right)^2\right]\right\}+\frac{\sigma}{(\rho c)_f}(uB-E)^2 \tag{10}$$

Using the order of magnitude analysis for the momentum equations which is normal to the stretching sheet and boundary layer approximation [36], expressed as follows:

$u \square v$

$\frac{\partial u}{\partial y} \square \frac{\partial u}{\partial x}, \frac{\partial v}{\partial t}, \frac{\partial v}{\partial x}, \frac{\partial v}{\partial y}$

(11)

$$\frac{\partial p}{\partial y}=0$$

Subsequently of the approximation and analysis, the governing equations (1)-(5) reduced to the following set presented as:

$$\frac{\partial u}{\partial x}+\frac{\partial v}{\partial y}=0 \tag{12}$$

$$\frac{\partial u}{\partial t}+u\frac{\partial u}{\partial x}+v\frac{\partial u}{\partial y}=-\frac{1}{\rho_f}\frac{\partial p}{\partial x}+v\left(\frac{\partial^2 u}{\partial y^2}\right)+\frac{\sigma}{\rho_f}\left(EB-uB^2\right)+$$
$$\frac{1}{\rho_f}\left[(1-\varphi_\infty)\rho_{f\infty}\beta_T(T-T_\infty)+(\rho_p-\rho_{f\infty})\beta_\varphi(\varphi-\varphi_\infty)\right]g \tag{13}$$

$$\frac{\partial T}{\partial t}+u\frac{\partial T}{\partial x}+v\frac{\partial T}{\partial y}=\frac{k}{(\rho c)_f}\left(1+\frac{16\sigma^* T_\infty^3}{3k^* k}\right)\left(\frac{\partial^2 T}{\partial y^2}\right)+\frac{\mu}{(\rho c)_f}\left(\frac{\partial u}{\partial y}\right)^2+$$
$$\tau\left\{D_B\left(\frac{\partial \varphi}{\partial y}\frac{\partial T}{\partial y}\right)+\frac{D_T}{T_\infty}\left(\frac{\partial T}{\partial y}\right)^2\right\}+\frac{\sigma}{(\rho c)_f}(uB-E)^2 \tag{14}$$

$$\frac{\partial \varphi}{\partial t}+u\frac{\partial \varphi}{\partial x}+v\frac{\partial \varphi}{\partial y}=D_B\left(\frac{\partial^2 \varphi}{\partial y^2}\right)+\frac{D_T}{T_\infty}\left(\frac{\partial^2 T}{\partial y^2}\right)-k_1(\varphi-\varphi_\infty) \tag{15}$$

The resulted equations are converted into the dimensionless form by employing the following dimensionless quantities.

$$\psi=\sqrt{\frac{b\nu}{1-at}}xf(\eta),\quad \eta=y\sqrt{\frac{b}{\nu(1-at)}},\quad \theta=\frac{T-T_\infty}{T_w-T_\infty},$$
$$\phi=\frac{\varphi-\varphi_\infty}{\varphi_\infty},\quad T=T_\infty+T_0\frac{bx}{2\nu(1-at)^2} \tag{16}$$

The stream function ψ can be defined as:

$$u=\frac{\partial \psi}{\partial y},\qquad v=-\frac{\partial \psi}{\partial x}, \tag{17}$$

The equations of the momentum, the energy and the nanoparticle concentration are given in dimensionless form, after using equations (16)-(17) into equations (12)-(15) become:

$$f'''+ff''-f'^2-\delta\left(f'+\frac{\eta}{2}f''\right)+M\left(E_1-f'\right)+Gr\theta+Gm\phi=0 \tag{18}$$

$$\frac{1}{\Pr}\left(1+\frac{4}{3}Rd\right)\theta''+f\theta'-2f'\theta-\delta\left(\frac{\eta}{2}\theta'+2\theta\right)+Nb\theta'\phi'+Nt\theta'^2+Ecf''^2+ \tag{19}$$
$$MEc\left(f'-E_1\right)^2=0$$

$$\phi''+\frac{Nt}{Nb}\theta''+Lef\phi'-Le\delta\frac{\eta}{2}\phi'-Le\gamma\phi=0 \tag{20}$$

The boundary conditions are given by

$$f=s,\quad f'=1,\quad \theta=1,\quad Nb\phi'+Nt\theta'=0,\quad \text{at}\quad \eta=0,$$
$$f'=0,\quad \theta=0,\quad \phi=0,\quad \text{as}\quad \eta\to\infty, \tag{21}$$

Here $f', \theta,$ and ϕ is the velocity, the temperature, and the concentration in dimensionless respectively, $\delta=a/b$ the unsteadiness parameter, $Gr=g\beta_T(1-\varphi_\infty)\rho_{f\infty}(T_w-T_\infty)l/u_w^2\rho_f$ is the Grashof number, $Gm=g\beta_\varphi(\rho_p-\rho_{f\infty})\varphi_\infty l/u_w^2\rho_f$ is the mass Grashof number, $X=x/l$ is the dimensionless constant, $\Pr=\upsilon/\alpha$ stand for Prandtl number, $Nb=(\rho c)_p D_B\varphi_\infty/(\rho c)_f\upsilon$ is the Brownian motion parameter, $Le=\nu/D_B$ is the Lewis, $Nt=(\rho c)_p D_T(T_w-T_\infty)/(\rho c)_f\upsilon T_\infty$ denotes the thermophoresis parameter, $M=\sigma B_0^2/b\rho_f$ associates with magnetic field parameter, $E_1=E_0/u_w B_0$ is the electric field parameter, $Ec=u_w^2/c_p(T_w-T_\infty)$ is the Eckert number, $s=v_0/\sqrt{\nu b}$ is the suction $(s>0)$ /injection $(s<0)$ parameter and $Rd=4\sigma^* T_\infty^3/k^* k$ is the radiation parameter, $\gamma=k_0/b$ is the chemical reaction, for $\gamma>0$ associates to destructive chemical reaction while $\gamma<0$ corresponds to generative chemical reaction respectively. Where prime represents differentiation with respect to η. In our present study, the selection of non-dimensional embedded parameters of nanofluids is considered to vary in view of the works of [7, 11, 14, 36-38]. The present study is tight in the following aforementioned investigations with water as base fluid [38].

The skin friction coefficient and the local Nusselt number:

$$c_f=\frac{\tau_w}{\rho u_w^2(x,t)},\qquad Nu=\frac{xq_w}{k(T_w-T_\infty)}, \tag{22}$$

Where

$$\tau_w=\mu_f\left(\frac{\partial u}{\partial y}\right)_{y=0},\quad q_w=-\left(\left(k+\frac{16\sigma^* T_\infty^2}{3k^*}\right)\frac{\partial T}{\partial y}\right)_{y=0}, \tag{23}$$

Here τ_w depicts the shear stress due to the stretching surface, q_w associated with surface heat flux, $\mathrm{Re}=u_w l/\nu$ represents the Reynolds number and k is the thermal conductivity of the nanofluid. For the local skin-friction coefficient and local Nusselt number are presented in non-dimensional form as:

$$\mathrm{Re}^{1/2}c_f=f''(0),\qquad Nu/\mathrm{Re}^{1/2}=-\left(1+\frac{4}{3}Rd\right)\theta'(0), \tag{24}$$

3. Results and discussion

The set of highly nonlinear ordinary differential equations (18)-(20) with boundary conditions (21) are solved numerically for the different scale of values of physical emerging parameters such as magnetic field M, electric field E_1, suction/injection parameter s, Grashof number Gr, thermal radiation Rd, the mass Grashof number Gm, Eckert number Ec, unsteadiness parameter δ, Brownian motion parameter Nb, thermophoresis parameter Nt, Lewis number Le, and chemical reaction parameter γ. Numerical results were achieved through implicit finite difference scheme known as Keller box method detailed description of the method see [32]. For the validation of present numerical scheme, the results are presented and examined with [36] in some limiting case when $E_1 = \delta = Gm = Gr = 0$. The numerical values are in good agreement as displayed from Tables 1 presents the effects of emerging parameters on the skin friction coefficient.

Table 1: Comparison of Skin friction coefficient $-f''(0)$ when $Gm = Gr = 0$ for few values of $M, s, E_1,$ and δ.

M	s	E_1	δ	Ref [36]	Present results
0	0.5	0	0	1.2808	1.280777
0.5				1.5000	1.500000
1.0				1.6861	1.686141
1.5				1.8508	1.850781
2.0				2.0000	2.000000
1.0	0			1.4142	1.414214
	0.2			1.5177	1.517745
	0.7			1.8069	1.806880
	1.0			2.0000	2.000000
	0.2	0.1		-	1.335083
		0.3		-	1.003660
		0.5		-	0.698797
		0.1	0.2	-	1.400699
			0.7	-	1.547543
			1.5	-	1.774626

The influence of electric field parameter E_1 on the water base nanofluid velocity profile is displayed in Figure 2. In this figure, electric field parameter is an increasing function, the momentum boundary layer thickness rises proximate the plate with small amount of flow but rises far from the surface stretching sheet immensely as result of Lorentz force. The higher electric parameter associated with stronger Lorentz force and the subordinate electric parameter agrees to the weaker Lorentz force. This Lorentz force increases the nanofluid flow which induces the flow field to rise by reducing the frictional resistance. The electric field serves as accelerating force which enhances the nanofluid flow due to the stretching sheet away from the plate. The Figure depicts effects of magnetic field parameter M on the velocity profile. It is noticed from Figure 3 that the nanofluid velocity and momentum boundary layer thickness decreased for higher values of magnetic field M at the initial stage and after some distance away from the plate it increases due to the stretching sheet. The magnetic field parameter contains the Lorentz force, in which it possesses the ability to resist and accelerate the nanofluid flow due to the presence of electric field parameter. As such retardation in the nanofluid flow induces a reduction in the velocity field. The Lorentz force corresponds with the magnetic field leads to thinner the boundary layer thickness. In Figure 4 demonstrated the impact of unsteadiness parameter δ on the nanofluid velocity profile. Increasing in the values of δ pointers to diminution in the fluid velocity with the hydrodynamics boundary layer thickness. The velocity gradient increases with an increase in unsteadiness parameter. The influence of Grashof number Gr on the water base nanofluid velocity profile is depicted in Figure 5. It is noticeable that the velocity of the nanofluid increases with the increase of Grashof number. It leads to rising in momentum boundary layer thickness and the velocity profiles. In Figure 6, associates with mass Grashof number Gm on the nanofluid velocity sketch. The nanofluid velocity decreases with an intensification with mass Grashof number. It leads to thinner momentum boundary layer thickness and decreased in the velocity profiles. Figure 7 established the power of suction parameter $(s > 0)$ on the nanofluid velocity distribution. It is worth noticing that as the values of suction parameter increase, the rate of the velocity and momentum boundary layer thickness decreases. The velocity gradient tends to enhance the nanofluid flow and thicken the momentum boundary layer thickness. Opposite behavior occurred in the case of injection parameter $(s < 0)$.

Radiative heat transfer on the nanofluid temperature distribution is revealed in Figure 8. Higher values of thermal radiation parameter Rd enhances the rate of heat flux from the stretching sheet which induces rise to the nanofluid temperature. Hence the temperature field thermal boundary layer thickness increases with an increase in radiative heat transfer. The influence of Eckert number Ec on the nanofluid temperature distribution is unveiled in Figure 9. The nanofluid temperature increase for rise in the values of Eckert number. There is kinetic energy to enthalpy which enhances the temperature and thermal boundary layer thickness. The heat transfer rate at the stretching sheet surface reduces as viscous dissipation rises. The impact of Grashof number Gr on temperature distribution is designated in Figure 10. The nanofluid temperature decreases with the increase in Grashof number, induced thinner thermal boundary layer thickness. The increase in Grashof number resulted in the increase the heat transfer rate at the stretching sheet surface. In Figure 11, described the flow behavior of unsteadiness parameter δ on the nanofluid temperature profile. In this Figure the temperature decreases as the magnitude of the unsteadiness parameter increase. The reason is that the heat transfer rate rises with boosting in the unsteadiness parameter which results in decreases in the nanofluid temperature and thermal boundary layer thickness. The temperature gradient increases for higher values of unsteadiness parameter.

Effects of Brownian motion parameter Nb on nanoparticles concentration is sketched in Figure 12. The nanoparticles concentration decreased significantly for small values of Brownian motion to higher values. An increase in Brownian motion leads to the reduction in the nanoparticles concentration and solutal boundary layer thickness. Figure 13 illustrates the influence of thermophoresis parameter Nt on the nanoparticles concentration. It has an opposite fluid flow behavior to that of Brownian motion and its associated solutal boundary layer depth. It enhances the concentration and thickens the solutal boundary layer thickness for higher values of thermophoresis parameter. The effects of Lewis number Le on the concentration field is confirmed in Figure 14. The nanoparticles concentration field reduced significantly for higher values of Lewis number. Why because the lessening in the field and solutal boundary thickness is as result of a revolution in Brownian diffusion coefficient. Higher Lewis number related to fragile Brownian diffusion coefficient. The effects of mass Grashof number Gm on the concentration field is portrayed in Figure 15. The nanoparticle volume concentration increases with the increase in mass Grashof number, induced thicker solutal boundary layer thickness. Figure 16 exposed the influence of unsteadiness parameter δ on the concentration profile. It has a similar behavior to that of Figure 4. In Figure 17 revealed the effects of γ on the nanoparticle concentration profile. In this Figure, the concentration profiles enhanced with increasing values of $(\gamma < 0)$. The nanoparticle concentration and solutal boundary layer thickness enhance with generative chemical reaction $(\gamma < 0)$, and opposite trend is observed for destructive chemical reaction $(\gamma > 0)$. The presence of destructive reaction leads to conversion of the species, which reduces the solutal boundary layer thickness. The generative chemical reaction shows the species

diffuses from the linear stretching sheet in the free stream. Therefore, the solutal boundary layer thickness enhanced with a generative chemical reaction.

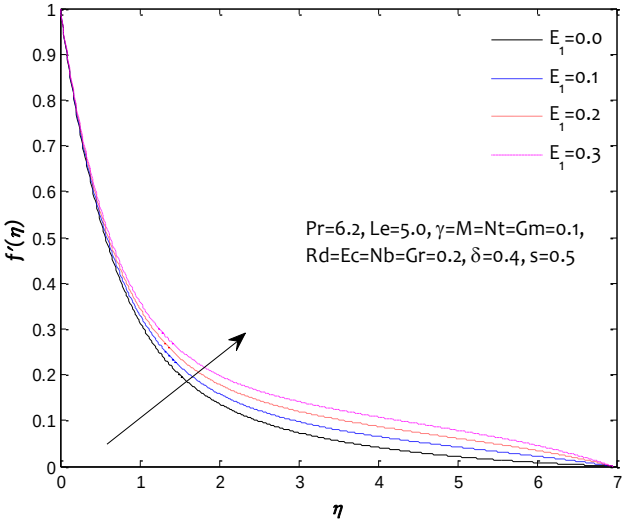

Figure 2: Influence of E_1 on the velocity profile

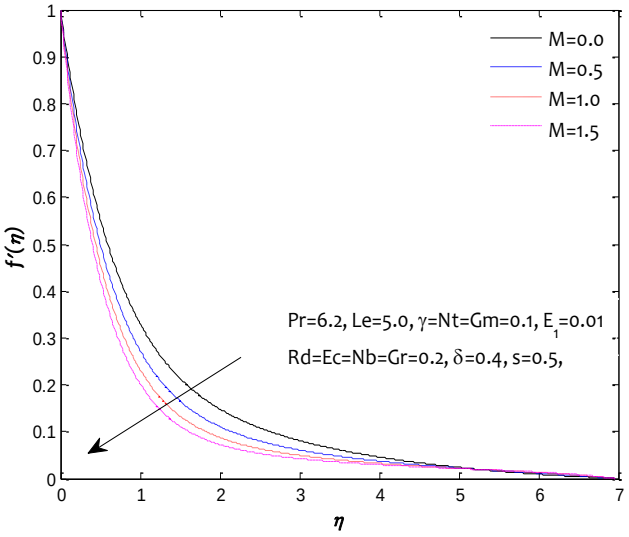

Figure 3: Influence of M on the velocity profile

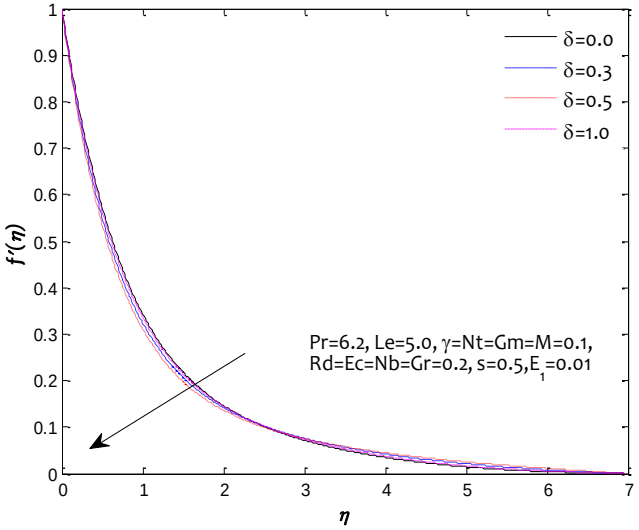

Figure 4: Influence of δ on the velocity profile

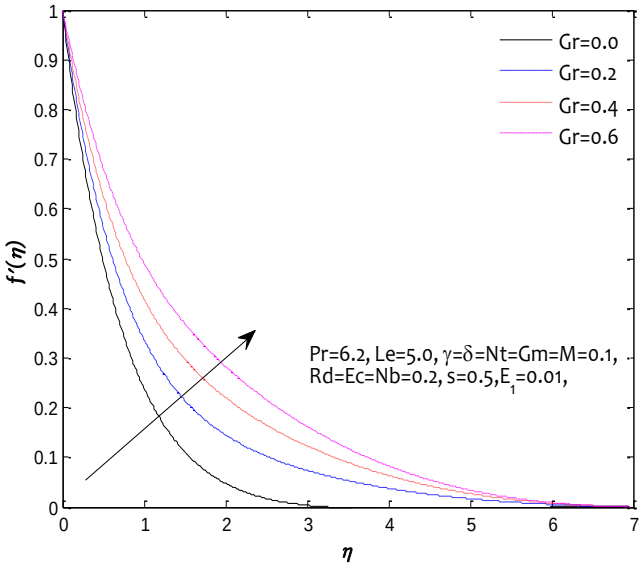

Figure 5: Influence of Gr on the velocity profile

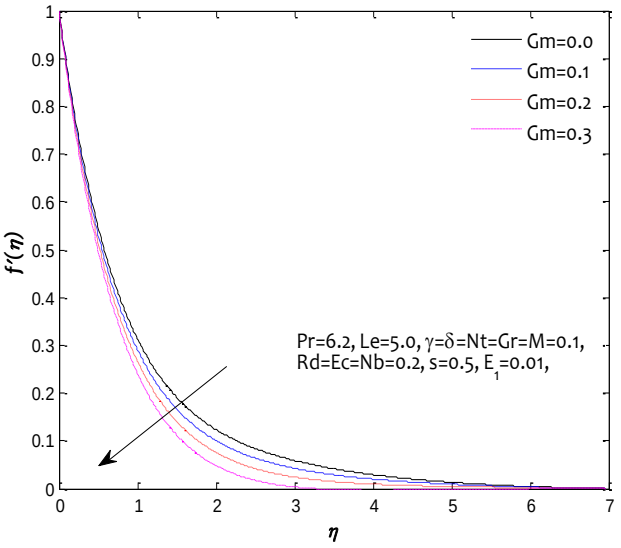

Figure 6: Influence of Gm on the velocity profile

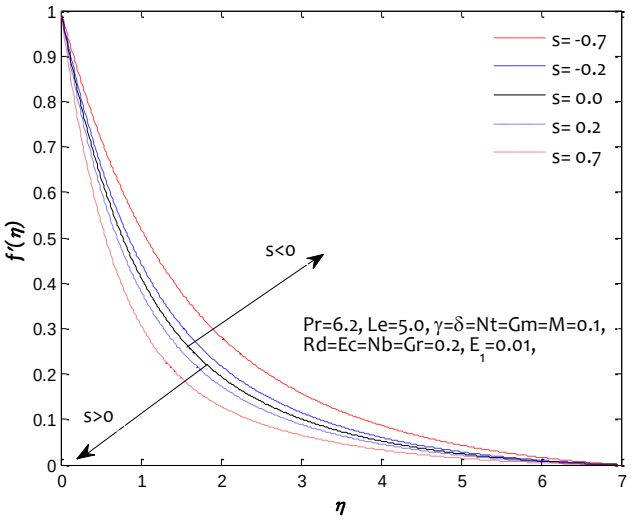

Figure 7: Influence of s on the velocity profile

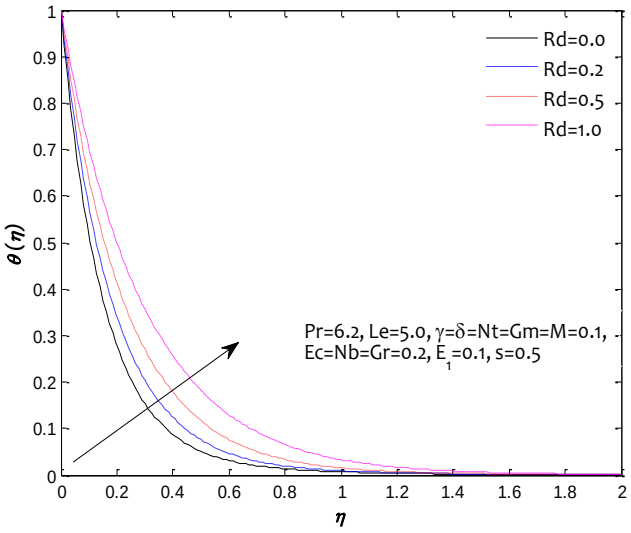

Figure 8: Influence of Rd on the temperature profile

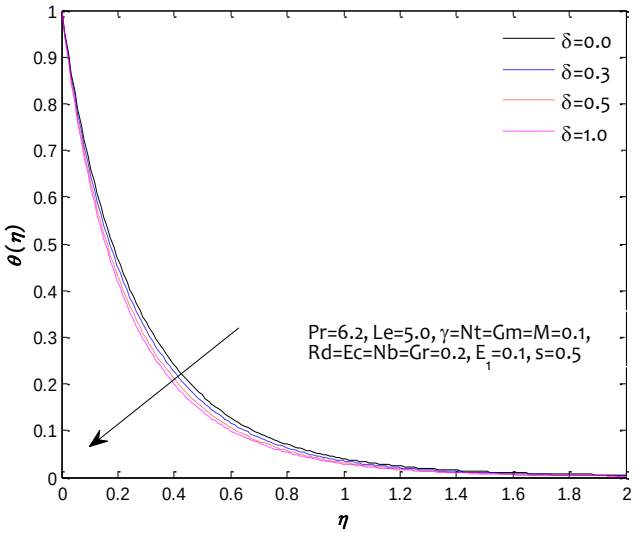

Figure 11: Influence of δ on the temperature profile

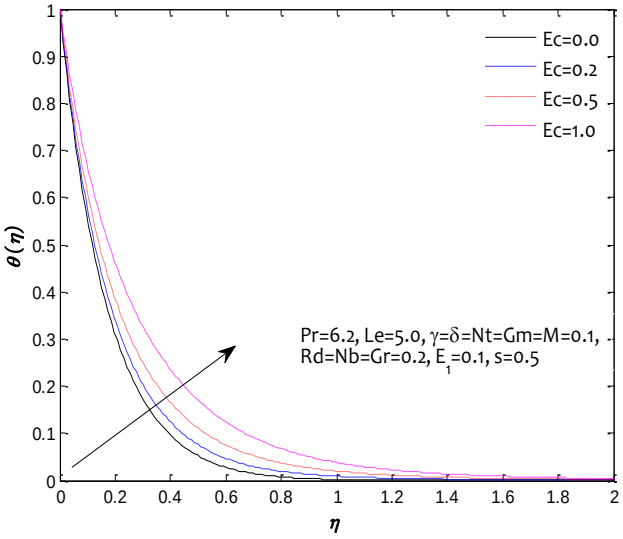

Figure 9: Influence of Ec on the temperature profile

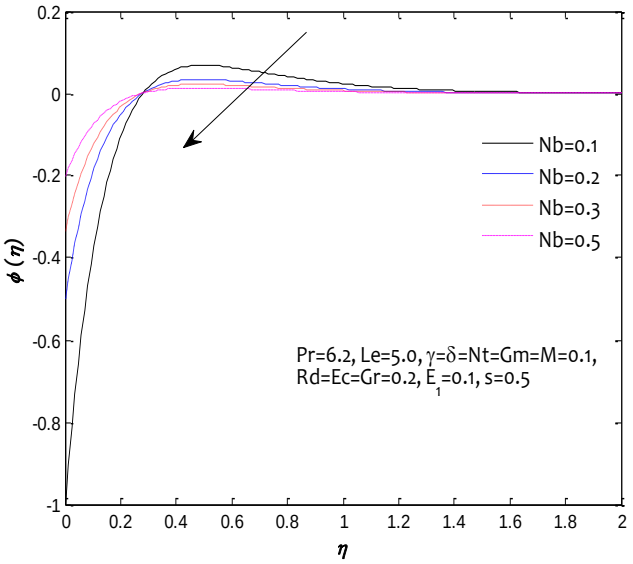

Figure 12: Influence of Nb on the concentration profile

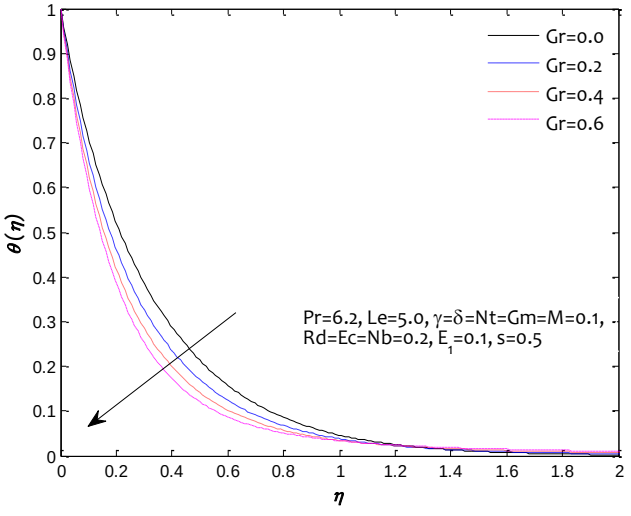

Figure 10: Influence of Gr on the temperature profile

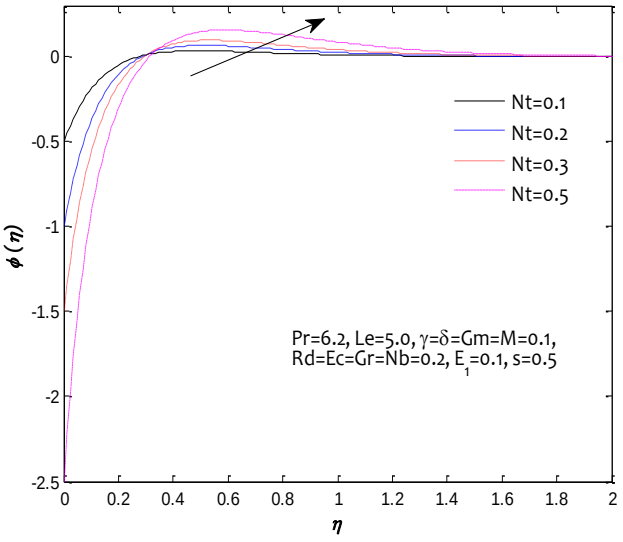

Figure 13: Influence of Nt on the concentration profile

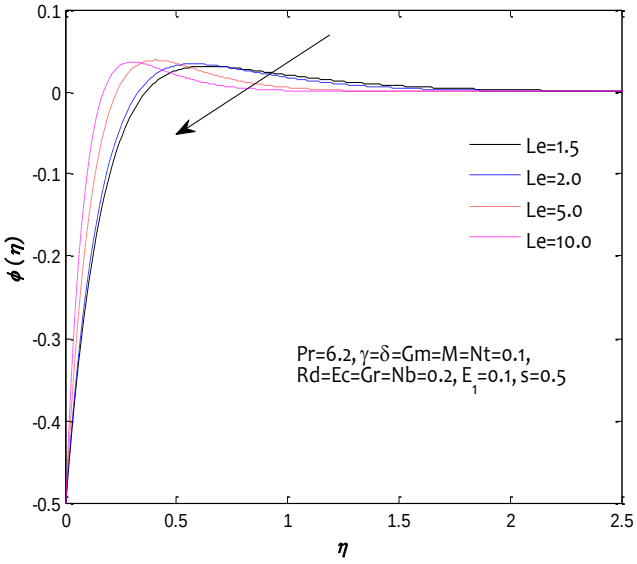

Figure 14: Influence of Le on the concentration profile

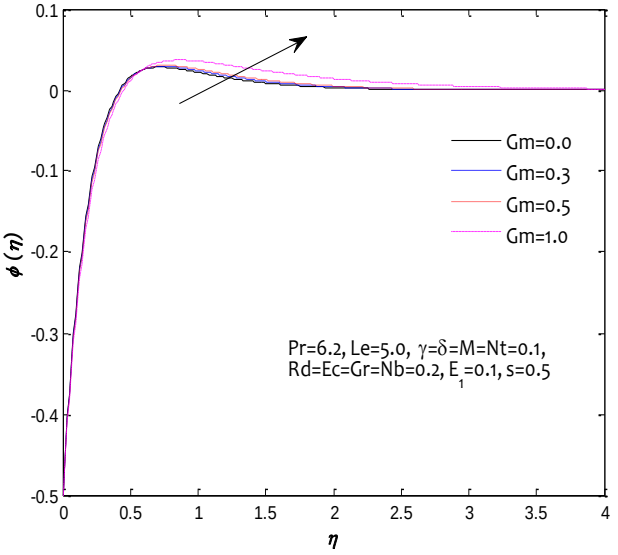

Figure 15: Influence of Gm on the concentration profile

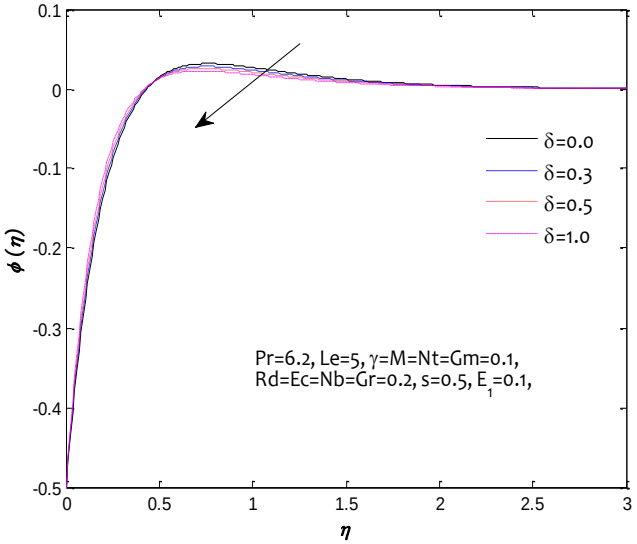

Figure 16: Influence of δ on the concentration profile

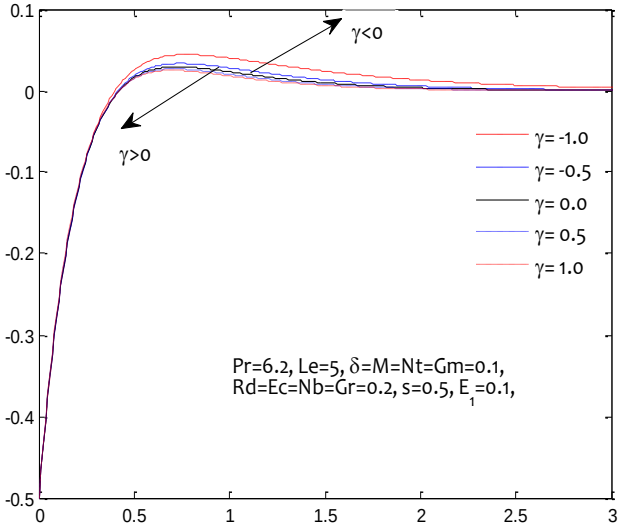

Figure 17: Influence of γ on the concentration profile

4. Conclusion

In this study, we have investigated the combined effects of viscous dissipation, and chemical reaction with thermal radiation on unsteady electrical magnetohydrodynamics (MHD) natural convective flow and heat transfer of nanofluid induced by the linear permeable stretching sheet. The numerical solution has been reported for the model under the influence of electric field E_1, magnetic field M, suction/injection parameter s, thermal radiation Rd, Eckert number Ec, unsteadiness parameter δ, Brownian motion parameter Nb, thermophoresis parameter Nt, Lewis number Le, and chemical reaction parameter γ, which are captured using implicit finite difference scheme. The significant velocity is achieved for a high amount of electric field, whereas the magnitude of velocity is suppressed by the magnetic field. Suction and Injection exhibits a reverse flow behavior on the velocity profiles. The rate of radiative heat transfer and viscous dissipation enhance the fluid temperature and thermal boundary layer thickness becomes thicker. The Grashof number increases with velocity and decreases with temperature, whereas mass Grashof number decreases with velocity and increases with concentration profiles. Unsteadiness parameter reduces the velocity, temperature and concentration profiles and Lewis decrease concentration distribution. Brownian motion and thermophoresis exhibit a reversed effects on the nanoparticle concentration profiles. The nanoparticles concentration enhance with generative chemical reaction and opposite trend occurs for destructive chemical reaction.

Acknowledgement

The authors would like to acknowledge Ministry of Higher Education and Research Management Centre, UTM for the financial support through vote numbers 13H28 and 03G53 for this research.

References

[1] Choi S, (1995), "S. Enhancement thermal conductivity of fluids with nanoparticles [J]," ed: ASME Publications.

[2] Ebrahimnia-Bajestan E, Moghadam M. C, Niazmand H, Daungthongsuk W, & Wongwises S, (2016), "Experimental and numerical investigation of nanofluids heat transfer characteristics for application in solar heat exchangers," *International Journal of Heat and Mass Transfer*, 92, pp. 1041-1052.

[3] Kakaç S, & Pramuanjaroenkij A, (2016), "Single-phase and two-phase treatments of convective heat transfer enhancement with nanofluids–a state-of-the-art review," *International Journal of Thermal Sciences*, 100, pp. 75-97.

[4] Kasaeian A., Daneshazarian R., Mahian O., Kolsi L., Chamkha A. J., Wongwises S., & Pop I, (2017), "Nanofluid flow and heat transfer in porous media: a review of the latest developments," *International Journal of Heat and Mass Transfer*, 107, pp. 778-791.

[5] Sundar LS, Sharma K, Singh MK, & Sousa A, (2017), "Hybrid nanofluids preparation, thermal properties, heat transfer and friction factor–A review," *Renewable and Sustainable Energy Reviews*, vol. 68, pp. 185-198.

[6] Abbasi FM, Shehzad SA, Hayat T, & Ahmad B, (2016) "Doubly stratified mixed convection flow of Maxwell nanofluid with heat generation/absorption," (in English), *Journal of Magnetism and Magnetic Materials*, 404, pp. 159-165.

[7] Buongiorno J, (2006) "Convective transport in nanofluids," *Journal of Heat Transfer*, 128(3), pp. 240-250.

[8] De P, Pal D, Mondal H, & Bera UK, (2017) "Effect of Thermophoresis and Brownian Motion on Magnetohydrodynamic Convective-Radiative Heat and Mass Transfer of a Nanofluid Over a Nonlinear Stretching Sheet," *Journal of Nanofluids*, vol. 6, no. 1, pp. 164-172.

[9] Hsiao K.-L., "Stagnation electrical MHD nanofluid mixed convection with slip boundary on a stretching sheet," *Applied Thermal Engineering*, vol. 98, pp. 850-861, 2016.

[10] Kuznetsov A, & Nield D, (2013) "The Cheng–Minkowycz problem for natural convective boundary layer flow in a porous medium saturated by a nanofluid: a revised model," *International Journal of Heat and Mass Transfer*, vol. 65, pp. 682-685.

[11] Makinde O, & Animasaun I, (2016) "Thermophoresis and Brownian motion effects on MHD bioconvection of nanofluid with nonlinear thermal radiation and quartic chemical reaction past an upper horizontal surface of a paraboloid of revolution," *Journal of Molecular liquids*, vol. 221, pp. 733-743.

[12] Daniel YS, (2015), "Presence of heat generation/absorption on boundary layer slip flow of nanofluid over a porous stretching sheet," *American Journal of Heat and Mass Transfer*, vol. 2, no. 1, pp. 15-30.

[13] Sheikholeslami M, Gerdroodbary MB, & Ganji D, (2017), "Numerical investigation of forced convective heat transfer of Fe-water nanofluid in the presence of external magnetic source," *Computer Methods in Applied Mechanics and Engineering*, vol. 315, pp. 831-845.

[14] Kandasamy R, Muhaimin I, & Mohamad R, (2013), "Thermophoresis and Brownian motion effects on MHD boundary-layer flow of a nanofluid in the presence of thermal stratification due to solar radiation," *International Journal of Mechanical Sciences*, vol. 70, pp. 146-154.

[15] Khan JA, Mustafa M, Hayat T, Farooq MA, Alsaedi A, & Liao S, (2014), "On model for three-dimensional flow of nanofluid: An application to solar energy," *Journal of Molecular Liquids*, vol. 194, pp. 41-47.

[16] Mustafa M, (2017), "MHD nanofluid flow over a rotating disk with partial slip effects: Buongiorno model," *International Journal of Heat and Mass Transfer*, vol. 108, pp. 1910-1916.

[17] Mushtaq A, Mustafa M, Hayat T, & Alsaedi A, (2014), "Nonlinear radiative heat transfer in the flow of nanofluid due to solar energy: A numerical study," *Journal of the Taiwan Institute of Chemical Engineers*, vol. 45, no. 4, pp. 1176-1183.

[18] Besthapu P, Haq RU, Bandari S, & Al-Mdallal QM, (2017), "Mixed convection flow of thermally stratified MHD nanofluid over an exponentially stretching surface with viscous dissipation effect," *Journal of the Taiwan Institute of Chemical Engineers*, vol. 71, pp. 307-314.

[19] Daniel YS, (2016), "Laminar Convective Boundary Layer Slip Flow over a Flat Plate using Homotopy Analysis Method," *Journal of The Institution of Engineers (India): Series E*, vol. 97, no. 2, pp. 115-121.

[20] Hayat T, Khan MI, Waqas M, Alsaedi A, & Yasmeen T, (2016), "Diffusion of chemically reactive species in third grade flow over an exponentially stretching sheet considering magnetic field effects," *Chinese Journal of Chemical Engineering*, vol. 25, no. 3, pp. 257-263..

[21] Krishnamurthy M, Prasannakumara B, Gireesha B, & Gorla RSR, (2016), "Effect of chemical reaction on MHD boundary layer flow and melting heat transfer of Williamson nanofluid in porous medium," *Engineering Science and Technology, an International Journal*, vol. 19, no. 1, pp. 53-61.

[22] Metri PG, Abel MS, & Silvestrov S, (2016), "Heat and Mass Transfer in MHD Boundary Layer Flow over a Nonlinear Stretching Sheet in a Nanofluid with Convective Boundary Condition and Viscous Dissipation," in *Engineering Mathematics I*: Springer, pp. 203-219.

[23] Nandeppanavar MM, Abel MS, & Kemparaju M, (2017), "Stagnation Point Flow, Heat and Mass Transfer of MHD Nanofluid Due to Porous Stretching Sheet Through Porous Media with Effect of Thermal Radiation," *Journal of Nanofluids*, vol. 6, no. 1, pp. 38-47.

[24] Daniel YS, Aziz ZA, Ismail Z, & Salah F, (2017), "Effects of thermal radiation, viscous and Joule heating on electrical MHD nanofluid with double stratification," *Chinese Journal of Physics*, vol. 55, no. 3, pp. 630-651.

[25] Daniel YS, Aziz ZA, Ismail Z, & Salah F, (2017), "Entropy analysis in electrical magnetohydrodynamic (MHD) flow of nanofluid with effects of thermal radiation, viscous dissipation, and Chemical reaction," *Theoretical and Applied Mechanics Letters*, vol. 7, no. 4, pp. 235-242.

[26] Daniel YS, (2015) "Steady MHD Laminar Flows and Heat Transfer Adjacent to Porous Stretching Sheets using HAM," *American Journal of Heat and Mass Transfer*, vol. 2, no. 3, pp. 146-159.

[27] Daniel YS, Aziz ZA, Ismail Z, & Salah F, (2017), "Effects of slip and convective conditions on MHD flow of nanofluid over a porous nonlinear stretching/shrinking sheet," *Australian Journal of Mechanical Engineering*, pp. 1-17.

[28] Daniel YS, Aziz ZA, Ismail Z, & Salah F, (2017), "Impact of thermal radiation on electrical MHD flow of nanofluid over nonlinear stretching sheet with variable thickness," *Alexandria Engineering Journal*, https://doi.org/10.1016/j.aej.2017.07.007.

[29] Daniel YS, (2017), "MHD Laminar Flows and Heat Transfer Adjacent to Permeable Stretching Sheets with Partial Slip Condition," *Journal of Advanced Mechanical Engineering*, vol. 4, no. 1, pp. 1-15.

[30] Daniel YS, (2016), "Steady MHD Boundary-layer Slip Flow and Heat Transfer of Nanofluid over a Convectively Heated of a Non-linear Permeable Sheet," *Journal of Advanced Mechanical Engineering*, vol. 3, no. 1, pp. 1-14.

[31] Daniel YS, Aziz ZA, Ismail Z, & Salah F, (2017), "Journal of Applied Research and Technology," *Journal of Applied Research and Technology*, vol. 15, pp. 464-476.

[32] Cebeci T, & Bradshaw P, *Physical and computational aspects of convective heat transfer*. Springer Science & Business Media, 1988.

[33] Hayat T, Shafiq A, & Alsaedi A, (2014), "Effect of Joule heating and thermal radiation in flow of third grade fluid over radiative surface," *Plos one*, vol. 9, no. 1, p. e83153.

[34] Pal D, & Mondal H, (2010), "Hydromagnetic non-Darcy flow and heat transfer over a stretching sheet in the presence of thermal radiation and Ohmic dissipation," *Communications in Nonlinear Science and Numerical Simulation*, vol. 15, no. 5, pp. 1197-1209.

[35] Daniel YS, & Daniel SK, (2015), "Effects of buoyancy and thermal radiation on MHD flow over a stretching porous sheet using homotopy analysis method," *Alexandria Engineering Journal*, vol. 54, no. 3, pp. 705-712.

[36] Ibrahim W, & Shankar B, (2013), "MHD boundary layer flow and heat transfer of a nanofluid past a permeable stretching sheet with velocity, thermal and solutal slip boundary conditions," *Computers & Fluids*, vol. 75, pp. 1-10.

[37] Khan W & Pop I, (2010) "Boundary-layer flow of a nanofluid past a stretching sheet," *International journal of heat and mass transfer*, vol. 53, no. 11, pp. 2477-2483.

[38] Mabood F, Khan W, & Ismail AM, (2015) "MHD boundary layer flow and heat transfer of nanofluids over a nonlinear stretching sheet: a numerical study," *Journal of Magnetism and Magnetic Materials*, vol. 374, pp. 569-576.